Article

Current Biology

The Earliest Stages of Mitochondrial Adaptation to Low Oxygen Revealed in a Novel Rhizarian

Highlights

- Microaerobic *B. motovehiculus* mitochondria are metabolically versatile
- A transitional organelle combines mitochondrial and hydrogenosomal attributes
- Aerobic metabolism is degenerating, with loss and fragmentation of key genes
- This work is a window into the evolutionary adaptation of mitochondria to low oxygen

Authors

Ryan M.R. Gawryluk, Ryoma Kamikawa, Courtney W. Stairs, Jeffrey D. Silberman, Matthew W. Brown, Andrew J. Roger

Correspondence

andrew.roger@dal.ca

In Brief

Gawryluk et al. report a complex transitional organelle that reveals key links between mitochondria and hydrogenosomes. Their investigation points to a general model of adaptation to life at low oxygen via loss and degeneration of critical aerobic genes, in concert with lateral gene transfer-mediated acquisition of anaerobic metabolism.

Gawryluk et al., 2016, Current Biology *26*, 1–10
October 24, 2016 Crown Copyright © 2016 Published by Elsevier Ltd.
http://dx.doi.org/10.1016/j.cub.2016.08.025

CellPress

Please cite this article in press as: Gawryluk et al., The Earliest Stages of Mitochondrial Adaptation to Low Oxygen Revealed in a Novel Rhizarian, Current Biology (2016), http://dx.doi.org/10.1016/j.cub.2016.08.025

Current Biology
Article

The Earliest Stages of Mitochondrial Adaptation to Low Oxygen Revealed in a Novel Rhizarian

Ryan M.R. Gawryluk,[1,2,9] Ryoma Kamikawa,[3,4] Courtney W. Stairs,[1,2] Jeffrey D. Silberman,[5] Matthew W. Brown,[6,7] and Andrew J. Roger[1,2,8,10,*]
[1]Department of Biochemistry and Molecular Biology, Dalhousie University, Halifax, NS B3H 4R2, Canada
[2]Centre for Comparative Genomics and Evolutionary Bioinformatics, Department of Biochemistry and Molecular Biology, Dalhousie University, Halifax, NS B3H 4R2, Canada
[3]Graduate School of Human and Environmental Studies, Kyoto University, Kyoto 606-8501, Japan
[4]Graduate School of Global Environmental Studies, Kyoto University, Kyoto 606-8501, Japan
[5]Department of Biological Sciences, University of Arkansas, Fayetteville, AR 72701, USA
[6]Department of Biological Sciences, Mississippi State University, Mississippi State, MS 39762, USA
[7]Institute for Genomics, Biocomputing and Biotechnology, Mississippi State University, Mississippi State, MS 39762, USA
[8]Program in Integrated Microbial Biodiversity, Canadian Institute for Advanced Research, Halifax, NS B3H 4R2, Canada
[9]Present address: Department of Botany, University of British Columbia, Vancouver, BC V6T 1Z4, Canada
[10]Lead Contact
*Correspondence: andrew.roger@dal.ca
http://dx.doi.org/10.1016/j.cub.2016.08.025

SUMMARY

Mitochondria exist on a functional and evolutionary continuum that includes anaerobic mitochondrion-related organelles (MROs), such as hydrogenosomes. Hydrogenosomes lack many classical mitochondrial features, including conspicuous cristae, mtDNA, the tricarboxylic acid (TCA) cycle, and ATP synthesis powered by an electron transport chain (ETC); instead, they produce ATP anaerobically, liberating H_2 and CO_2 gas in the process. However, our understanding of the evolutionary transformation from aerobic mitochondria to various MRO types remains incomplete. Here we describe a novel MRO from a cercomonad (*Brevimastigomonas motovehiculus* n. sp.; Rhizaria). We have sequenced its 30,608-bp mtDNA and characterized organelle function through a combination of transcriptomic, genomic, and cell biological approaches. *B. motovehiculus* MROs are metabolically versatile, retaining mitochondrial metabolic pathways, such as a TCA cycle and ETC-driven ATP synthesis, but also possessing hydrogenosomal-type pyruvate metabolism and substrate-level phosphorylation. Notably, the *B. motovehiculus* ETC is degenerate and appears to be losing cytochrome-based electron transport (complexes III and IV). Furthermore, the F_1F_o ATP synthase (complex V) is unique, with the highly conserved Atpα subunit fragmented into four separate pieces. The *B. motovehiculus* MRO appears to be in the process of losing aerobic metabolic capacities. Our findings shed light on the transition between organelle types, specifically the early stages of mitochondrial adaptation to anaerobiosis.

INTRODUCTION

Mitochondria derive from the integration of an ancient α-proteobacterial endosymbiont within a host cell related to the Lokiarchaeota lineage of Archaea [1]. All eukaryotes described thus far, except *Monocercomonoides* species [2], possess mitochondria or their anaerobic derivatives, broadly termed mitochondrion-related organelles (MROs), indicating that they were present in the last common ancestor of extant eukaryotes. This fact has spawned considerable interest in untangling the events surrounding the origin of mitochondria, which some investigators have hypothesized to be the seminal event in the genesis of eukaryotic cells [3, 4].

Mitochondria are most famous as the major site of aerobic oxidative phosphorylation (OXPHOS), the O_2-dependent synthesis of ATP via the coupled electron transport chain (ETC) and F_1F_o ATP synthase (complex V [CV]). However, facultatively anaerobic mitochondria have been described in animals that, under low oxygen conditions, generate ATP by substrate-level phosphorylation via succinyl-CoA synthetase (SCS) and acetate:succinate CoA-transferase (ASCT), employing alternative terminal electron acceptors, such as fumarate [5]. Furthermore, metabolically streamlined MROs have evolved independently in diverse microbial eukaryotes that inhabit low O_2 environments [6]. Several of these MROs, such as hydrogenosomes and mitosomes, lack classical mitochondrial features such as mtDNA, the pyruvate dehydrogenase complex (PDH), the tricarboxylic acid (TCA) cycle, and the ETC. Rather, MROs such as hydrogenosomes decarboxylate pyruvate via an O_2-sensitive enzyme, pyruvate:ferredoxin oxidoreductase (PFO), to generate acetyl-CoA and CO_2. Electrons from this reaction are passed to a ferredoxin, which is then reoxidized by an [FeFe]-hydrogenase

that reduces protons to produce H_2 gas. ATP is generated via substrate-level phosphorylation, essentially as in anaerobic mitochondria [7].

Although the common ancestry of mitochondria and hydrogenosomes was not initially apparent, the subsequent identification of classical mitochondrial proteins targeted to MROs [8], along with conserved components of the protein import machinery [9], provided strong evidence for their common origin. However, it was the characterization of functionally intermediate organelles between mitochondria and hydrogenosomes that shed light on the evolutionary transitions between organelle types. For instance, the aerobic mitochondria of the amoebozoan *Acanthamoeba castellanii* [10, 11] also possess enzymes characteristic of hydrogenosomes, presumably enabling ATP production in both aerobic and anaerobic conditions [12]. These organelles represent the starting point in the transition from mitochondria into hydrogenosomes. Furthermore, anaerobic H_2-producing mitochondria (HPMs) have been described in the ciliate, *Nyctotherus ovalis*, and the stramenopile, *Blastocystis* species [13, 14]. HPMs in these species retain some mitochondrial features like mtDNA, an incomplete TCA cycle, a partial ETC that lacks complexes III and IV (CIII and CIV), and the capacity to generate ATP via CV. Instead, these HPMs generate ATP by the hydrogenosomal-type pathway and are therefore functional intermediates between mitochondria and hydrogenosomes. Yet, there is still much to learn about the initial steps in the transition from classical mitochondria to MROs. This is because *A. castellanii* mitochondria are essentially classical mitochondria that have acquired hydrogenosomal metabolism (i.e., they are not reduced [11]), whereas HPMs are already substantially functionally simplified [13, 14].

Employing a combination of genomic, transcriptomic, microscopic, and cell biological approaches, we report a novel microaerophilic cercomonad, *Brevimastigomonas motovehiculus* n. sp., a member of the eukaryotic supergroup Rhizaria. While *B. motovehiculus* MROs resemble hydrogenosomes ultrastructurally, metabolic reconstructions indicate that they are mitochondria in the earliest stages of degeneration, and they represent an important snapshot of the evolutionary transition from an O_2-respiring mitochondrion to an HPM.

RESULTS AND DISCUSSION

B. motovehiculus Possesses Hydrogenosome-like Organelles with Reduced mtDNA

In agreement with light microscopic findings (Figure 1A; Figure S1; see Text S1 for taxonomic summary), maximum-likelihood (ML) and Bayesian phylogenetic analyses of 18S rRNA sequences (Figure S2A) robustly placed *B. motovehiculus* as a close relative of the facultatively anaerobic cercomonad *Brevimastigomonas anaerobica* [15, 16].

Transmission electron microscopy (TEM) of *B. motovehiculus* revealed numerous small, oval bodies (typically 300–600 nm) distributed throughout the cell, often displaying double membranes (Figure 1B, lower right inset); these structures are likely MROs, consistent with their MitoTracker reactivity (Figure 1C). One or two distinct folds of the inner membrane were infrequently apparent, indicating the presence of very limited cristae (Figure 1B, upper right inset). Cristae are often absent from hydrogenosomes [17–19], but they are commonly observed in HPMs [20, 21]. Curiously, *B. motovehiculus* MROs have far fewer cristae than their counterparts in *B. anaerobica*, and they are enriched near the elongated nucleus instead of the cell's periphery [16]. This difference could be due to the fact that the *B. anaerobica* cells used for TEM were grown aerobically [16], in contrast to the *B. motovehiculus* cells presented here.

We identified and characterized a 30,608-bp circular-mapping mitochondrial genome in *B. motovehiculus* (Figure 1D). Genes encoding the small and large subunit rRNAs along with six tRNAs were identified, indicating that most tRNAs are imported from the cytosol. In total, nine genes encoding proteins of known function, subunits of ETC complexes I (CI), III, IV, and V, along with three unidentified open reading frames (ORFs) $\geq$100 amino acids in length were identified in *B. motovehiculus* mtDNA. The presence of encoded ETC proteins on this mtDNA suggests the potential to generate ATP using OXPHOS. However, the sequence of the putative apocytochrome *b* (Cob; CIII) homolog was extraordinarily divergent (Figure S3A) as was the Cox1 protein sequence; Cox1 was missing several of the amino acids required for proton pumping, although all copper- and heme-coordinating His residues were conserved (Figure S3B). This list of mtDNA-encoded proteins was not sufficient to determine if the ETC in *B. motovehiculus* MROs produces ATP through classical OXPHOS. To better characterize the functions of these MROs, we assembled an inventory of nucleus-encoded, MRO-targeted proteins using a transcriptomic approach.

A Typical Protein Import Apparatus Functions in *B. motovehiculus* MROs

The mitochondrial protein import apparatus directs proteins with N-terminal or internal targeting sequences (MTSs) into mitochondria. *B. motovehiculus* encodes subunits of the outer membrane translocase (TOM complex), the sorting and assembly machinery complex (SAM), the presequence-dependent import pathway mediated by the TIM23 complex, the mitochondrial carrier protein import pathway (TIM22 complex), and the mitochondrial processing peptidase (Figure 2A). The number of protein import machinery components identified in *B. motovehiculus* is on par with reports from HPMs such as those of *Blastocystis* species subtypes 1 and 7 [13]. *B. motovehiculus* MROs are similarly capable of importing nucleus-encoded proteins bearing classical N-terminal MTSs.

B. motovehiculus MROs Have a Complex Proteome

As *B. motovehiculus* mtDNA encodes components of the mitochondrial translation system (tRNAs and rRNAs) and ETC, nucleus-encoded proteins for replication, transcription, and translation of mitochondrial genes, along with certain components of the ETC, must be targeted to the mitochondrial matrix. Consistent with this, the N termini of most *B. motovehiculus* proteins involved in the expression of mtDNA-encoded genes and the ETC possess classical MTSs ([22]; Figure S4). TargetP [23] and MitoProt [24] software tools confidently predicted the mitochondrial localization of these proteins (Table S1), validating this approach to identifying mitochondrial proteins in *B. motovehiculus*. Through in silico predictions, the *B. motovehiculus* MRO proteome was inferred to be complex, with >400 putative mitochondrial proteins identified in our transcriptomic analysis,

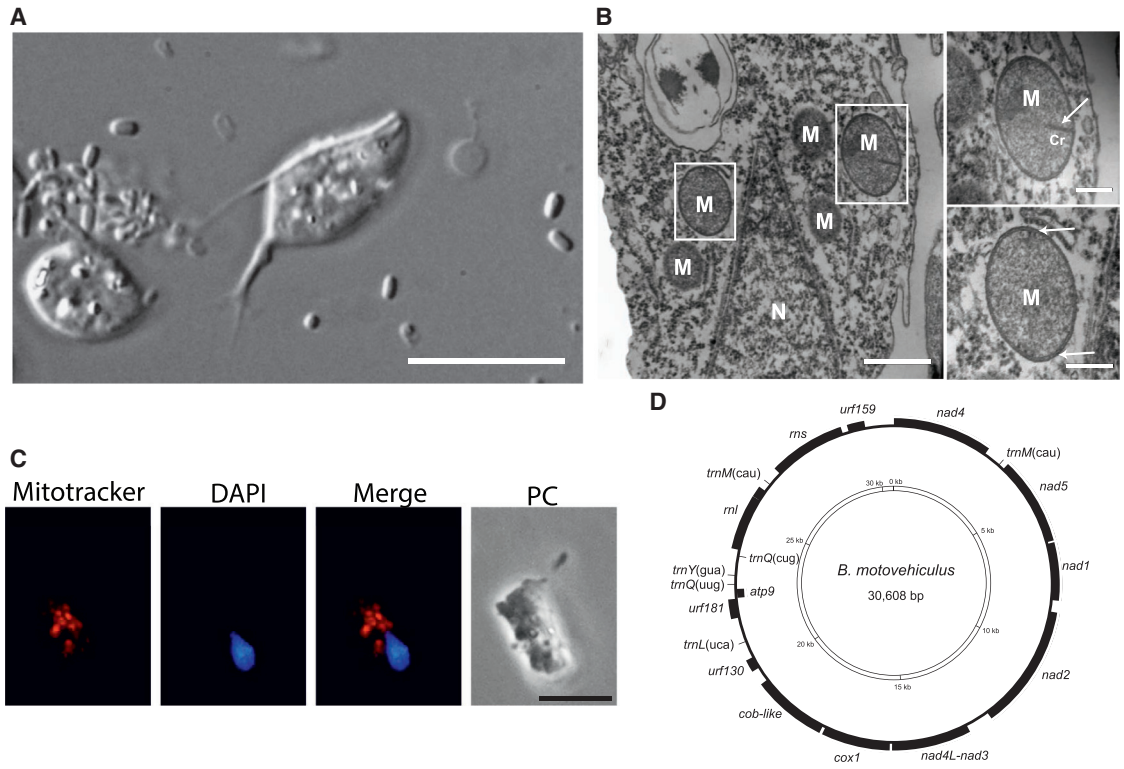

Figure 1. *B. motovehiculus* Contains MROs with Limited Cristae and a Reduced Mitochondrial Genome

(A) Differential interference contrast micrograph shows a *B. motovehiculus* cell.

(B) Transmission electron micrographs indicate hydrogenosome-like organelles. Mitochondria (M) and the nucleus (N) are labeled. The two inset images are of the boxed mitochondria in the first image, but at higher magnification. The arrow in the top image denotes the presence of a membrane invagination interpreted to be a single crista (Cr). Arrows in the bottom image demarcate the double membrane. Scale bars represent 500, 200, and 200 nm.

(C) *B. motovehiculus* MROs are MitoTracker reactive. *B. motovehiculus* MROs and DNA were co-stained with MitoTracker Orange and DAPI, respectively. The merged image shows that the MROs congregate near the nucleus, consistent with TEM images. The last panel shows a phase-contrast micrograph of the cell.

(D) Complete 30,608-bp mitochondrial genome of *B. motovehiculus*. Protein-coding and rRNA-coding genes are demarcated by black boxes; tRNA-coding genes are marked by black lines.

See also Text S1 and Figure S1.

including >20 metabolite transporters and enzymes associated with the metabolism of fatty acids, amino acids, Fe-S clusters, and nucleotides (Table S1). Of these transcripts, each is represented to some degree in our draft genome dataset, with ≥1 spliceosomal intron identified in 96% of the candidate genes. Below we describe the energy generation system of *B. motovehiculus* MROs.

A Degraded Proton-Pumping ETC in *B. motovehiculus*'s MROs

The *B. motovehiculus* nuclear genome encodes subunits of proton-pumping NADH dehydrogenase (CI), including components inherited from the bacterial ancestor of mitochondria and certain components invented within the eukaryotic domain [25] (Figure 2B). All of the subunits required for NADH oxidation and transfer of electrons to ubiquinone are accounted for [26]. Moreover, several conserved CI assembly factors were identified (Figure 2B), indicating that the complex is likely assembled in a fashion similar to canonical aerobic mitochondria. These MROs appear to house a fully functional proton-pumping CI.

All four subunits of succinate dehydrogenase (complex II [CII]; also a component of the TCA cycle), SdhA, SdhB, SdhC, and SdhD, are nucleus encoded in *B. motovehiculus*, and abundantly expressed (Table S1) and phylogenetic reconstructions of SdhA indicate that the *B. motovehiculus* homolog is of mitochondrial origin (Figure S2B). *B. motovehiculus* also encodes several conserved CII assembly factors, including Sdh5, Sdh7, and Sdh8, altogether indicating a functional CII.

In aerobic mitochondria, CIII oxidizes ubiquinol and subsequently reduces cytochrome *c*, which shuttles electrons from CIII to CIV. Cox2, a component of CIV, oxidizes cytochrome *c* and passes electrons to Cox1, which reduces O_2 to H_2O. No nucleus-encoded subunits or assembly factors of either CIII or CIV were identified in our RNA sequencing (RNA-seq) dataset, including catalytic subunits like Cox2 (typically mtDNA encoded). Given the divergent sequences of *cob* and *cox1* discussed above, CIII and CIV may not be capable of efficient electron transport and proton pumping, indicating that CI is likely the sole proton pump in the *B. motovehiculus* ETC. Genomic DNA contigs with genes encoding Qcr6, the Rieske Fe-S protein, cytochrome *c*1 (CIII subunits), Cox3 (CIV subunit), Cox11, Cox15 (CIV assembly factors), and cytochrome *c* were identified, but corresponding transcripts were absent in the RNA-seq data. The inferred protein sequences were often truncated and

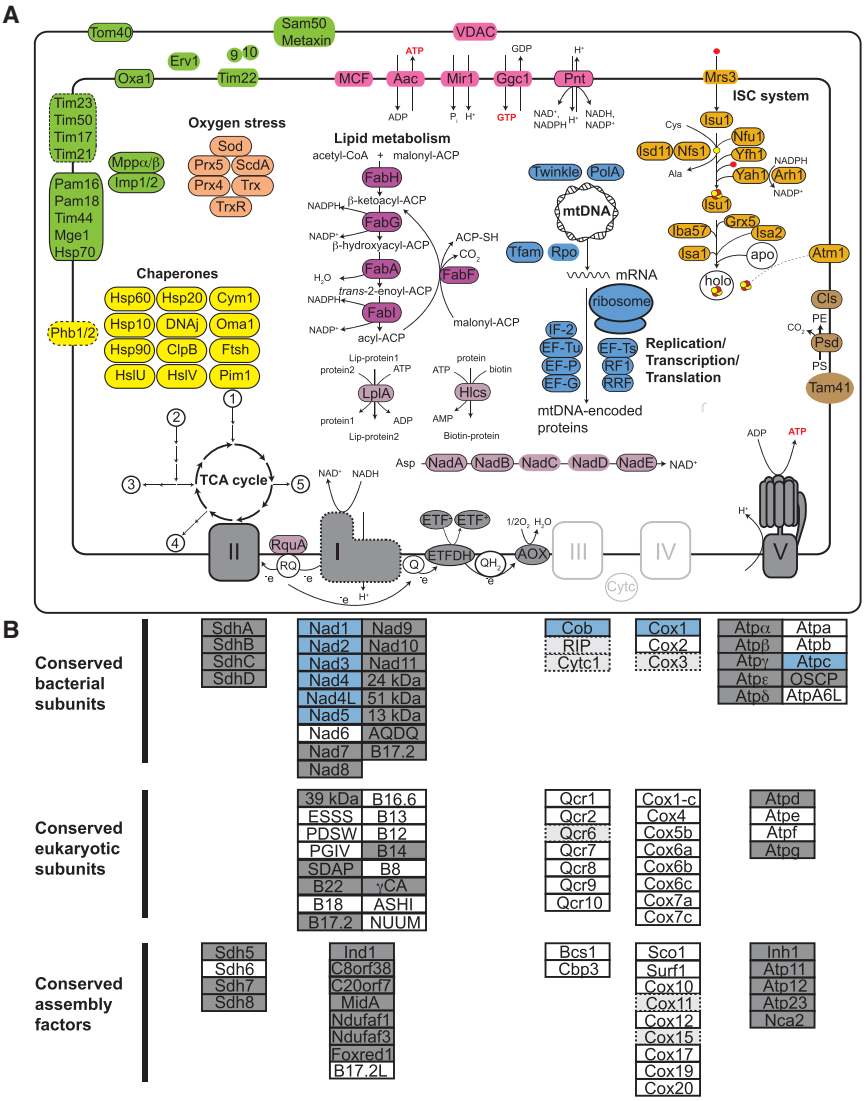

Figure 2. *B. motovehiculus* MROs Contain a Reduced ETC

(A) Metabolic reconstruction of *B. motovehiculus* MROs. Circled numbers drawn near the TCA cycle represent pathways presented in Figure 4. A subset of evolutionarily and functionally important proteins inferred to localize to *B. motovehiculus* mitochondria also is presented. See Table S1 for full protein names. Dotted lines refer to protein complexes in which only some of the subunits contain classical MTSs. I, NADH dehydrogenase; II, succinate dehydrogenase; III cytochrome *c* reductase; IV, cytochrome *c* oxidase; V, F_1F_o ATP synthase; TCA cycle, tricarboxylic acid cycle.

(B) Subunit composition of *B. motovehiculus* ETC complexes. Box shading is as follows: gray, nucleus-encoded subunits identified via RNA-seq; blue, mtDNA-encoded proteins; light gray with dashed line, partial draft genomic sequences; unshaded, not identified in our molecular datasets. Only subunits found in other cercozoans are depicted.

See also Table S1 and Figures S2–S4.

extremely divergent, suggesting that they might be nonfunctional pseudogenes (Figure 2B).

We also identified an MTS-bearing homolog of alternative oxidase (AOX), an enzyme that accepts electrons from ubiquinol. We suggest that *B. motovehiculus* uses AOX as a terminal acceptor for electrons derived from the catabolism of amino acids by mitochondrial flavoprotein dehydrogenases, such as the electron transfer flavoprotein and electron transfer flavoprotein-ubiquinone oxidoreductase (ETF and ETF-QO) [27]. We hypothesize that electrons from CI are used by CII to reduce fumarate (see below).

ATP Production through a Peculiar F_1F_o ATP Synthase

In aerobic mitochondria, protons pumped by the ETC are utilized for ATP production by the F_1F_o ATP synthase (CV). CV is composed of a membrane-embedded motor (F_o sector) and a matrix-associated F_1 sector that generates ATP via a rotational catalytic mechanism involving the α, β, and γ subunits. In addition to Atpc (mtDNA encoded), we have identified eight catalytic and/or structural nucleus-encoded subunits of CV, in addition to the five factors that regulate CV function (Inh1 and Nca2) and participate in the assembly of the F_o and F_1 sectors (Atp11, Atp12, and Atp23). *B. motovehiculus* appears to have retained the capacity to generate ATP via OXPHOS, in spite of its highly reduced cristae and degenerate CIII and CIV.

Most surprisingly, the F_1 Atpα subunit occurs in four distinct nucleus-encoded proteins that we refer to as Atpα1, Atpα2, Atpα3, and Atpα123, each unusually divergent (Figures 3A and 3B; Figure S5). The Atpα1 subunit aligns with the most N-terminal portion of classical Atpα, whereas the Atpα2 and Atpα3 polypeptides align with the central and most C-terminal portions, respectively. The Atpα123 subunit overlaps somewhat with the same portion of classical Atpα to which the Atpα1, Atpα2, and ATPα3 subunits collectively align, although it is extremely divergent. Notably, Atpα123 is expressed at lower levels than the other subunits (Table S1). We hypothesize that Atpα123 represents a severely degraded version of the ancestral Atpα protein.

Each inferred protein sequence includes a predicted N-terminal MTS, and we have demonstrated that these putative MTSs are sufficient for import of Atpα1-GFP, Atpα2-GFP, and Atpα3-GFP into yeast mitochondria (Figure 3A). Given that each of Atpα1, Atpα2, and Atpα3 overlap to some extent with Atpα123, it is expected that this would cause redundancy. In support of this, each of Atpα2 and Atpα123 has Walker A and B motifs, which are critical in classical ATPα for nucleotide binding. Notably, the Atpβ subunit, the binding partner of Atpα, is also unusual as it is three times larger than its counterparts in other mitochondria; but, it is less divergent and demonstrably mitochondrial in origin (Figure S2C).

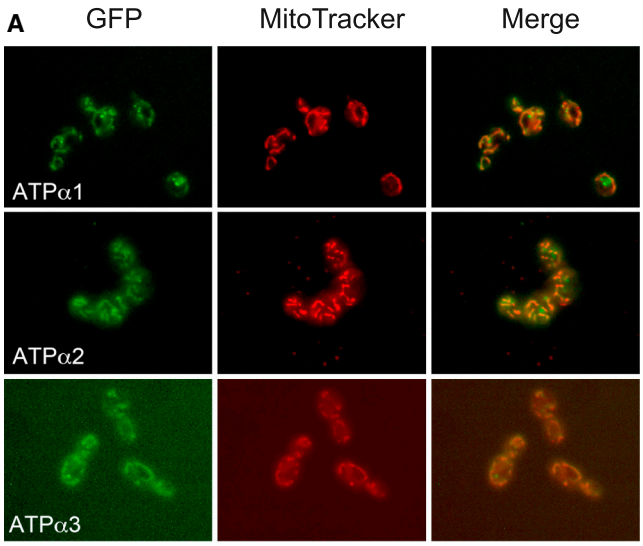

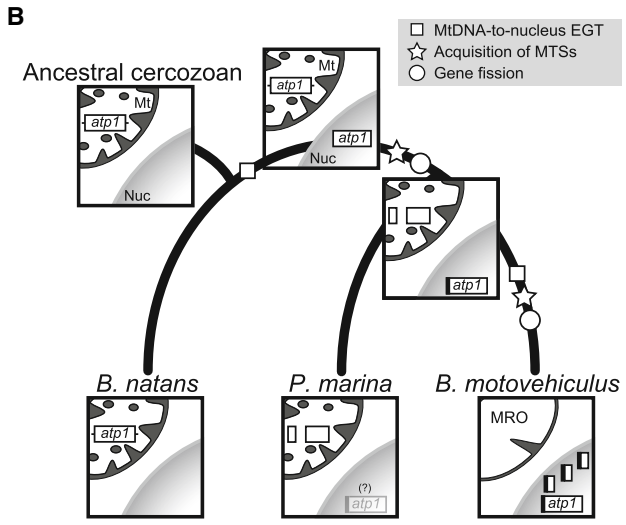

Figure 3. An Unusual F_1F_o ATP Synthase in *B. motovehiculus* MROs

(A) Localization of *B. motovehiculus* Atpα1, Atpα2, and Atpα3 GFP fusion proteins in yeast. Indicated GFP fusion proteins were expressed in yeast (green, GFP column). Mitochondria were co-stained with MitoTracker Orange (orange, MTR column). A merged image is presented in the right column.

(B) A proposed evolutionary scenario accounting for the unusual Atpα in cercomonads. Mitochondria (mt) and the nucleus (nuc) are depicted in the boxed image. Duplication, fission, and endosymbiotic gene transfer of *atp*1 resulted in a split mtDNA-encoded *atp*1 (white boxes) and MTS-bearing, nucleus-encoded *atp*1 in the common ancestor of *P. marina* + *B. motovehiculus*. Further gene duplications, fissions, transfers, and MTS acquisitions occurred in the lineage leading to *B. motovehiculus*.

See also Figures S4 and S5.

Although it is unclear how well CV could function with the otherwise highly conserved ATPα in such a fragmented state, numerous other examples of split mitochondrial proteins are known [28–30] that, in some cases, are enzymatically active [10, 29]. However, no known mitochondrial protein reported to date is as extensively fragmented as *B. motovehiculus* Atpα.

Atpα is encoded as a single polypeptide in the mtDNA of the cercozoans *Bigelowiella natans*, *Lotharella oceanica* [31], and *Spongospora subterranea* [32], but as two distinct proteins in the mtDNA of *Paracercomonas marina* (NC_026310.1). It is likely that the fission of *atp*α into two mitochondrial genes occurred after the divergence of *B. motovehiculus* and *P. marina* from other cercozoans, but before the divergence of *P. marina* and *B. motovehiculus* (Figure 3B). The Atpα1 subunit of *B. motovehiculus* is equivalent to the Atp1_a of *P. marina* (Figure S5). Likewise, Atpα2 aligns with the N-terminal portion of *P. marina* Atp1_b and Atpα3 aligns with the C-terminal part. Further gene duplication and fission events, along with gene transfer to the nucleus and acquisition of MTSs, must have occurred in the lineage leading to *B. motovehiculus* (Figure 3B).

A Complete TCA Cycle in *B. motovehiculus* MROs?

In aerobic mitochondria, the TCA cycle generates NADH, which fuels electron transport and proton pumping by CI. We have identified MTS-bearing homologs of all TCA cycle enzymes, except for citrate synthase (CS), in our RNA-seq dataset. However, a query of our genomic dataset revealed a contig encoding a mitochondrial-type CS homolog (not shown), though we were unable to determine if it is targeted to mitochondria. We hypothesize that the expression of CS is O_2 dependent and that the TCA cycle runs in the reductive (reverse) direction under anaerobic conditions; but, under increased O_2 concentrations, CS may be upregulated such that the classical oxidative TCA cycle predominates. Alternatively, it is possible that CS is a pseudogene in *B. motovehiculus*.

Consistent with a reductive TCA cycle functioning under hypoxia (Figure 4), we identified a homolog of RquA, a recently characterized methyltransferase that is necessary for the biosynthesis of rhodoquinone (RQ) from ubiquinone (UQ) [33, 34]. RQ is a low-redox-potential quinone that permits CII to operate efficiently in reverse as a fumarate reductase [35]. Like RquA in other eukaryotes [17], *B. motovehiculus* RquA may have been acquired laterally (Figure S2D). The predicted MTS of this protein promotes import into yeast mitochondria (Figure 5B), strongly suggesting that RQ is synthesized in *B. motovehiculus* MROs.

If an incomplete reverse TCA cycle predominates in anaerobic *B. motovehiculus* MROs, the nearly complete suite of enzymes expressed under anaerobic conditions is perplexing. This is because aconitase (ACO), for which citrate is a substrate, and isocitrate dehydrogenase, $NADP^+$-dependent isoform (ICDH) are expressed at levels comparable to the TCA cycle enzymes that comprise the reductive portion of the cycle (i.e., malate dehydrogenase, MDH; type I fumarase, FUM; succinate dehydrogenase, CII), although oxoglutarate dehydrogenase (OGDH) is expressed at lower levels (Table S1). To rationalize the expression of these enzymes under anaerobic conditions, we sought a mitochondrion-targeted enzyme capable of metabolizing citrate. We identified in *B. motovehiculus* a homolog of ATP citrate lyase (ACL; single-subunit type [36]), which catalyzes the ATP-dependent cleavage of citrate into acetyl-CoA and oxaloacetate. The reverse reaction is also energetically favorable and yields citrate and ATP through substrate-level phosphorylation.

Although ACL is localized to the cytosol in all organisms studied to date, the *B. motovehiculus* homolog has a clear 34–35 amino acid (aa) MTS relative to the highly conserved N terminus

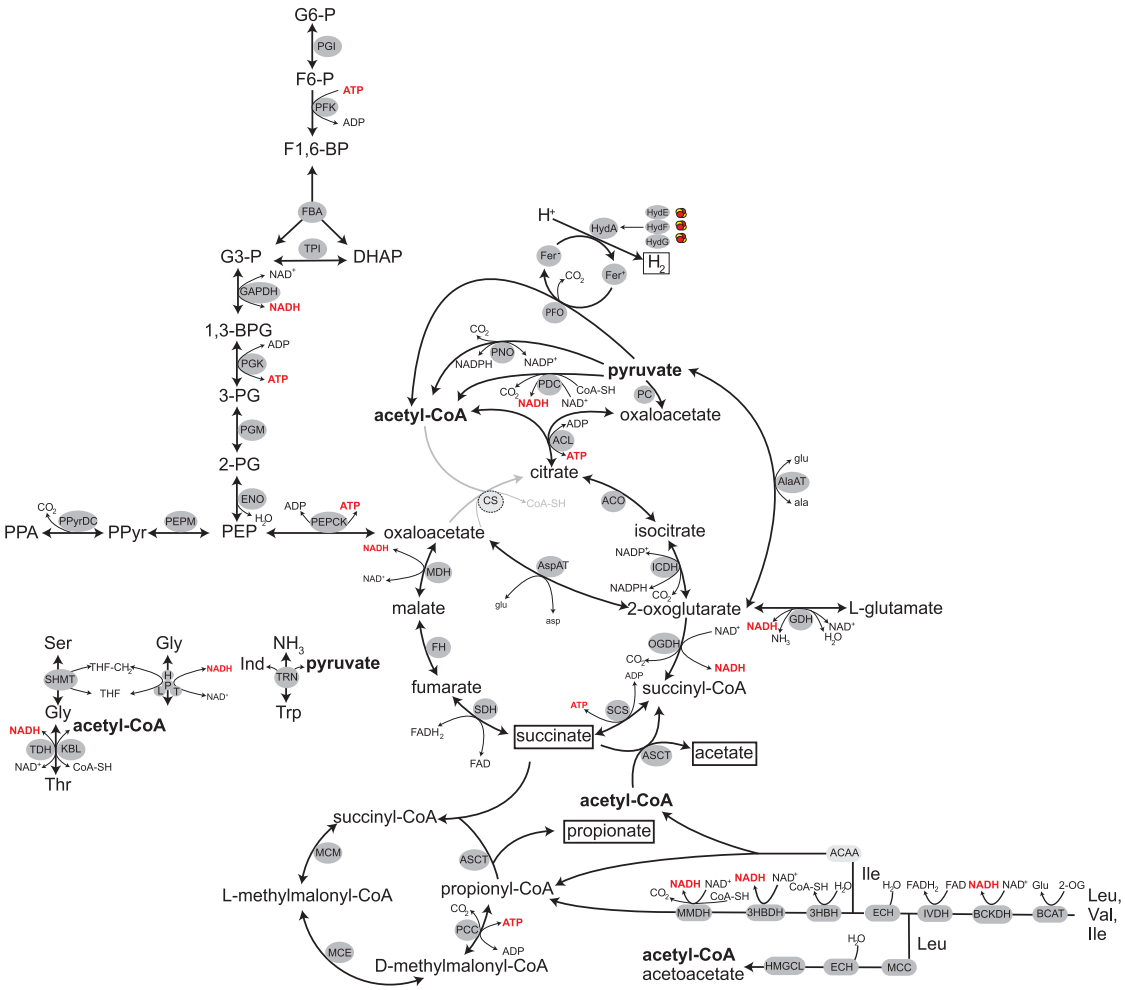

Figure 4. The Anaerobic *B. motovehiculus* TCA Cycle and Related Reactions

All TCA cycle reactions were identified in transcriptomic analyses, except for CS (reaction arrow shaded gray). We suggest that CS is repressed in anaerobic conditions and that ACL functions either as a citrate lyase or a citrate synthase under anaerobic conditions. All of the metabolic processes presented here are predicted to occur inside the MRO. Certain ATP- and NADH-generating reactions are marked in bold red; reactions that yield pyruvate and acetyl-CoA are bolded. Potential metabolic end products are boxed. See Table S1 for full protein names. See also Figure S4.

of ACL from other organisms. We suggest that this ACL operates in mitochondria as either (1) a citrate lyase or (2) a citrate synthase. If ACL is a citrate lyase, it would entail a reversal of the first steps of the classical TCA cycle. Although OGDH and the NAD-specific isoform of ICDH catalyze irreversible reactions, the less-studied NADP-specific isoform of ICDH, as present in *B. motovehiculus* mitochondria, also may be capable of synthesizing isocitrate from oxoglutarate [37, 38]. Since ACO is readily reversible, ACL could cleave the resulting citrate, yielding oxaloacetate that subsequently feeds into the reductive portion of the TCA cycle and acetyl-CoA for fatty acid synthesis or ATP production via SCS and ASCT. Alternatively, if ACL is a citrate synthase, it indicates that the *B. motovehiculus* TCA cycle is bifurcated under anaerobic conditions, with MDH, FUM, and CII acting reductively (with SCS generating ATP) and ACL, ACO, ICDH, and OGDH yielding oxoglutarate or succinyl-CoA for anaplerotic reactions, as well as NADH for CI function. The feasibility of our scenario is demonstrated by the report that ACL has replaced CS in the TCA cycle of *Desulfobacter postgatei* [39]. It is conceivable that the reversibility of ACL, in contrast to CS, may permit shifts in the direction of the *B. motovehiculus* TCA cycle during anaerobic growth, depending on physiological conditions. Unfortunately, due to the abundance and diversity of bacteria in the *B. motovehiculus* culture, it is not currently feasible to test these alternatives experimentally.

Coexistence of Mitochondrial and Hydrogenosomal Pyruvate Metabolism

Pyruvate is typically imported into mitochondria by the pyruvate carrier, MCP1/MCP2 [40], or generated within mitochondria by NAD-dependent malic enzyme, but we did not identify mitochondrion-targeted homologs of either. Notably, as in other rhizarians, stramenopiles, and alveolates [41–43], *B. motovehiculus* MROs are predicted to house a partial glycolytic pathway in addition to the cytosolic counterpart. However, phosphoenolpyruvate is the predicted end product and may be a substrate for

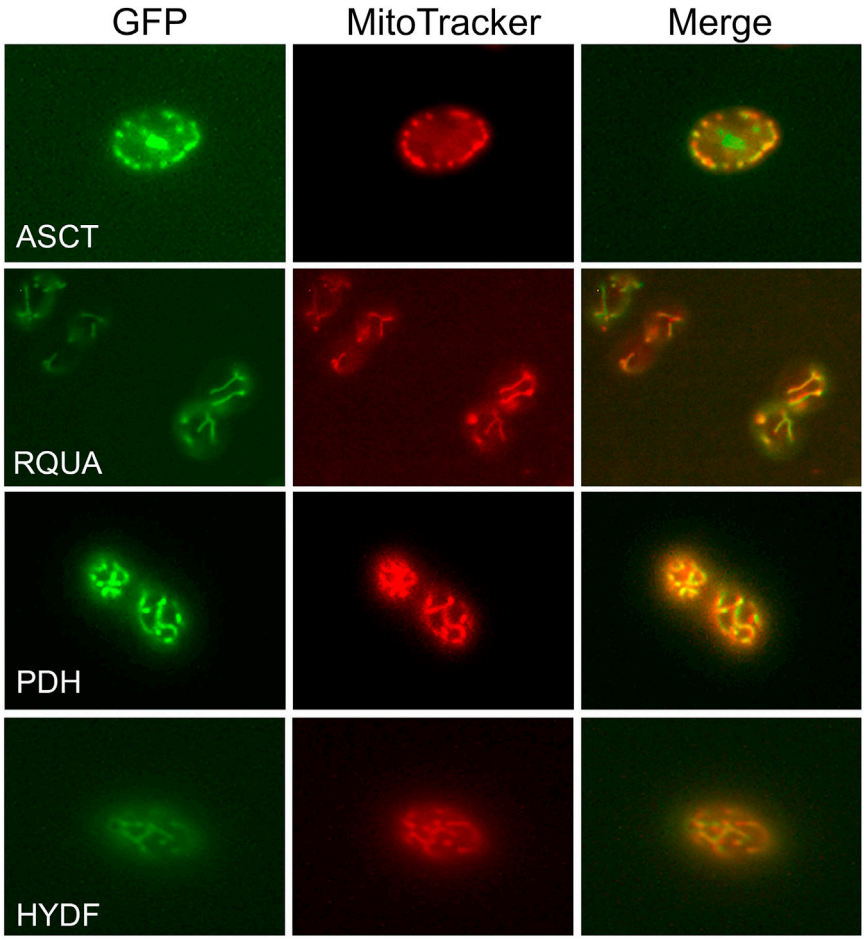

Figure 5. Subcellular Localization of Key *B. motovehiculus* Enzymes in Yeast

Columns depict yeast localization of *B. motovehiculus*-GFP constructs (GFP), MitoTracker dye (MitoTracker), and a merged image (Merge). ASCT, acetate:succinate CoA-transferase subfamily 1b protein (ASCT1b); RQUA, rhodoquinone biosynthesis gene A; PDH, pyruvate dehydrogenase E1β subunit; HYDF, Fe-hydrogenase assembly factor F. See also Figures S2 and S4.

aminophosphonate metabolism (Figure 4; Table S1). Two predicted MRO-targeted enzymes, alanine aminotransferase and tryptophanase, are capable of generating pyruvate (Figure 4).

In aerobic mitochondria, PDH converts pyruvate into acetyl-CoA and CO_2. In contrast, many anaerobic MROs utilize an O_2-sensitive enzyme, PFO. PFO transfers electrons to [Fe-Fe]-hydrogenase (HydA) via a ferredoxin carrier, generating H_2. Substrate-level synthesis of ATP/GTP is subsequently carried out in combination by ASCT and SCS, yielding succinate (and/or propionate) and acetate as metabolic end products [7].

We identified transcripts encoding all subunits of PDH in the RNA-seq data. Phylogenetic analysis of the E1β subunit confirmed its mitochondrial provenance (BS = 99, BPP = 1.0; Figure S2E). Furthermore, a *B. motovehiculus* E1β-GFP construct localized to yeast mitochondria (Figure 5C), providing further evidence that PDH functions in *B. motovehiculus* as it does in aerobic eukaryotes.

B. motovehiculus encodes eukaryotic-type homologs (Figure S2F) of PFO (three) and a related enzyme, pyruvate:$NADP^+$ oxidoreductase (PNO; two). Each possesses an N-terminal extension relative to prokaryotic homologs, and in silico predictions suggest that at least three have an MTS.

[Fe-Fe]-hydrogenase (HydA) transfers electrons from PFO-reduced ferredoxin to H^+, yielding H_2. Three assembly factors, HydE, HydF, and HydG, aid in the maturation of HydA's catalytic H-cluster; we identified eukaryotic-type single copies of each in *B. motovehiculus* (Figures S2G–S2I). The inferred HydA and HydF protein sequences confidently predicted MTSs, while HydE lacked a predicted MTS and the N terminus of HydG was not obtained (Table S1). Subcellular localization experiments in yeast demonstrated that a *B. motovehiculus* HydF-GFP construct is targeted to mitochondria (Figure 5).

B. motovehiculus encodes two ASCT1b family proteins, ASCT1b1 and ASCT1b2, which act in concert with SCS in various anaerobically functioning mitochondria and hydrogenosomes to generate ATP or GTP via substrate-level phosphorylation [44, 45]. Each of the ASCT1b1 and ASCT1b2 groups were within a poorly supported eukaryotic clade (Figure S2J). Both isoforms of ASCT1b had N-terminal extensions, and an ASCT1b1-GFP construct localized to yeast mitochondria (Figure 5). In addition, *B. motovehiculus* encodes mitochondrion-targeted methylmalonyl-CoA mutase, methylmalonyl-CoA epimerase, and propionyl-CoA carboxylase, which collectively transform succinate into propionate, yielding ATP in a similar manner to anaerobic mitochondria, HPMs, and other MROs [6, 7]. Together our data indicate the presence of all constituents of the hydrogenosomal energy generation pathway in *B. motovehiculus* mitochondria, and they predict that succinate, propionate, acetate, and H_2 are generated as end products (Figure 4).

Comparison of *B. motovehiculus* Mitochondria to Other MROs: Diversity and Evolution

Here we have shown that *B. motovehiculus* MROs blur the distinction between mitochondria and HPMs. Whereas hydrogenosomes lack the ETC altogether, HPMs from *N. ovalis* and *Blastocystis* species maintain reduced ETCs that include only CI and CII [13, 14], and ATP is generated through substrate-level phosphorylation. Our transcriptomic and genomic analyses suggest that *B. motovehiculus* CIII and CIV are functionally degraded, whereas CI, CII, and CV appear to be functional. ATP synthesis by CV (i.e., OXPHOS) has not been reported in any HPMs to date, although it may occur in hydrogenosomes of anaerobic fungi from the phylum *Neocallimastigomycota* [46, 47] (although, in the latter case, CV may function in reverse to create a proton

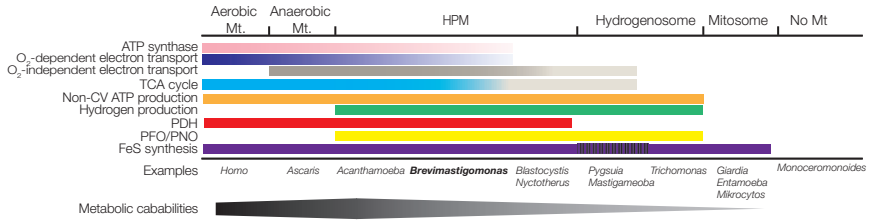

Figure 6. The Spectrum of Mitochondrial Function

Metabolic capabilities of various categories of MROs from diverse eukaryotes are presented. Solid boxes indicate functions that are present in a given MRO type; absence of a box indicates absence of function; faded portions of boxes indicate functional degradation; hatched lines on the *Pygsuia* and *Mastigamoeba* Fe-S cluster synthesis bar denotes replacement of the standard ISC system. Metabolic capacity is highest in pluripotent mitochondria (e.g., *Acanthamoeba*), with a full suite of aerobic and anaerobic ATP-generating machinery. *B. motovehiculus* MROs possess apparently degrading O_2-dependent (i.e., cytochrome-based) electron transport, ATP synthase (CV), and TCA cycle, thereby establishing a link between mitochondria and other anaerobic MROs.

gradient, since these organisms lack any proton-pumping ETC components). The emerging picture of the *B. motovehiculus* ETC is therefore of an intermediate between aerobic mitochondria and HPMs, and this provides a snapshot of the early stages of the adaptation of MROs to low-oxygen environments (Figure 6).

In aerobic mitochondria, acetyl-CoA is passed into the TCA cycle, which generates reducing equivalents and drives ATP synthesis via the ETC. In contrast, hydrogenosomes [48] lack the TCA cycle altogether. An intermediate scenario is observed in HPMs [7, 13, 14, 17]: the TCA cycle is incomplete, operating in a reductive fashion, yielding succinate (and/or propionate) and acetate. *B. motovehiculus* MROs possess a nearly complete or possibly complete TCA cycle, with the potential to function in either oxidative or reductive directions depending on environmental conditions (i.e., O_2 availability). This is reminiscent of TCA cycle function in the mitochondria of *Euglena gracilis* and parasitic helminths, which use RQ to permit CII to function as a fumarate reductase in anaerobic environments [7, 49].

Whereas aerobic and anaerobic mitochondria and hydrogenosomes decarboxylate pyruvate by PDH and PFO, respectively, some organisms, including *A. castellanii*, *Blastocystis* species, *N. ovalis*, and *B. motovehiculus*, employ both systems [11–14]. The co-existence of PDH and O_2-sensitive PFO affords a clear scenario for the transition from mitochondrial to hydrogenosomal pyruvate metabolism. Pyruvate catabolism in hydrogenosomes and HPMs is associated with H_2 production and ATP generation via ASCT and SCS. *B. motovehiculus* encodes homologs of each of these proteins, several of which we have demonstrated to localize to yeast mitochondria.

In combination with other recent reports [12–14, 17], our data further obscure the once sharp distinctions between mitochondria, HPMs, and hydrogenosomes, extending the notion that mitochondria exist on a phenotypic continuum [6] (Figure 6). Indeed, *B. motovehiculus* mitochondria likely mirror the early changes that MROs of other eukaryotic lineages must have traversed early in their adaptation to anaerobiosis [6]. The first steps that permitted invasion of novel anaerobic niches likely involved the lateral acquisition of genes encoding enzymes associated with anaerobic energy metabolism by an aerobe [6, 12], although the source(s) of these genes remains unresolved. Among these enzymes are PFO, HydA (and HydE-G), ASCT, and RquA. In response to low concentrations of O_2, expression of cytochrome-based electron transport components (CIII, CIV, and cytochrome *c*) is repressed. Concomitant downregulation of certain TCA cycle enzymes and synthesis of RQ from UQ by RquA favors a reductive TCA cycle. After such cells become increasingly adapted to living in low O_2, purifying selection on mtDNA- and nucleus-encoded genes associated with aerobic energy generation is relaxed. Uniquely, in *B. motovehiculus* mitochondria, we have caught the resulting sequence divergence (e.g., Cob, Cox1, and ATPα) and gene loss (possibly Cox2 and Qcr1) in the act.

Consistent with the metabolic repertoire of HPMs, our results suggest that CV may persist longer than CIII–CIV (Figure 6), taking advantage of the transmembrane proton motive force afforded by CI proton-pumping activity; it is, however, still unclear what factors favor the retention of CV, as CI is present in other HPMs lacking CV. One possibility is that the presence of a more complete TCA cycle in *B. motovehiculus*, along with other metabolic pathways that yield NADH, favors the retention of CV. In this scenario, the combined incomplete TCA cycle of HPMs (which consume NADH via MDH) and the remaining NADH-generating reactions do not generate sufficient NADH to establish robust proton gradients for efficient CV function. Rather, in *Blastocystis* and *Nyctotherus*, CI probably generates a transmembrane proton gradient sufficient for import of proteins and small molecules across the inner mitochondrial membrane. Additional systematic analyses exploring the links between reductive ETC evolution and NADH-generating metabolism in diverse MROs may provide further insight into the principles governing mitochondrial adaptation to anaerobiosis.

ACCESSION NUMBERS

The accession numbers for the raw reads data reported in this paper are NCBI SRA: SRP081237.

SUPPLEMENTAL INFORMATION

Supplemental Information includes five figures, a taxonomic summary, Supplemental Experimental Procedures, and one table and can be found with this article online at http://dx.doi.org/10.1016/j.cub.2016.08.025.

AUTHOR CONTRIBUTIONS

R.M.R.G., R.K., and C.W.S. performed experiments. M.W.B. and J.D.S. isolated *B. motovehiculus*. M.W.B. described and photographed *B. motovehiculus*. R.M.R.G., R.K., and A.J.R. wrote the manuscript. All authors read and approved the manuscript.

ACKNOWLEDGMENTS

This work, R.M.R.G., and C.W.S. were supported by operating grant MOP-142349 from the Canadian Institutes of Health Research (CIHR) awarded to

A.J.R. R.M.R.G. also was supported by a postdoctoral fellowship from the CIHR. This work was supported in part by grants from the Japan Society for Promotion of Science (JSPS 15H05606 and 15H14591 awarded to R.K.), the Arkansas Biosciences Institute (J.D.S.), and the National Science Foundation (DEB 1456054 awarded to M.W.B.). R.K. was supported by the JSPS Strategic Young Researcher Overseas Visits Program for Accelerating Brain Circulation. The authors thank Dr. Michelle Leger for helpful comments, along with Dr. Melanie Dobson, Joyce Chew, and Mary Ann Trevors for technical assistance.

Received: June 13, 2016
Revised: July 21, 2016
Accepted: August 9, 2016
Published: September 22, 2016

REFERENCES

1. Spang, A., Saw, J.H., Jørgensen, S.L., Zaremba-Niedzwiedzka, K., Martijn, J., Lind, A.E., van Eijk, R., Schleper, C., Guy, L., and Ettema, T.J.G. (2015). Complex archaea that bridge the gap between prokaryotes and eukaryotes. Nature *521*, 173–179.
2. Karnkowska, A., Vacek, V., Zubáčová, Z., Treitli, S.C., Petrželková, R., Eme, L., Novák, L., Žárský, V., Barlow, L.D., Herman, E.K., et al. (2016). A eukaryote without a mitochondrial organelle. Curr. Biol. *26*, 1274–1284.
3. Martin, W., and Müller, M. (1998). The hydrogen hypothesis for the first eukaryote. Nature *392*, 37–41.
4. Lane, N., and Martin, W. (2010). The energetics of genome complexity. Nature *467*, 929–934.
5. Tielens, A.G., Rotte, C., van Hellemond, J.J., and Martin, W. (2002). Mitochondria as we don't know them. Trends Biochem. Sci. *27*, 564–572.
6. Stairs, C.W., Leger, M.M., and Roger, A.J. (2015). Diversity and origins of anaerobic metabolism in mitochondria and related organelles. Philos. Trans. R. Soc. Lond. B Biol. Sci. *370*, 20140326.
7. Müller, M., Mentel, M., van Hellemond, J.J., Henze, K., Woehle, C., Gould, S.B., Yu, R.-Y., van der Giezen, M., Tielens, A.G.M., and Martin, W.F. (2012). Biochemistry and evolution of anaerobic energy metabolism in eukaryotes. Microbiol. Mol. Biol. Rev. *76*, 444–495.
8. Embley, T.M., van der Giezen, M., Horner, D.S., Dyal, P.L., and Foster, P. (2003). Mitochondria and hydrogenosomes are two forms of the same fundamental organelle. Philos. Trans. R. Soc. Lond. B Biol. Sci. *358*, 191–201, discussion 201–202.
9. Dolezal, P., Likic, V., Tachezy, J., and Lithgow, T. (2006). Evolution of the molecular machines for protein import into mitochondria. Science *313*, 314–318.
10. Gawryluk, R.M.R., Chisholm, K.A., Pinto, D.M., and Gray, M.W. (2012). Composition of the mitochondrial electron transport chain in *acanthamoeba castellanii*: structural and evolutionary insights. Biochim. Biophys. Acta *1817*, 2027–2037.
11. Gawryluk, R.M.R., Chisholm, K.A., Pinto, D.M., and Gray, M.W. (2014). Compositional complexity of the mitochondrial proteome of a unicellular eukaryote (*Acanthamoeba castellanii*, supergroup Amoebozoa) rivals that of animals, fungi, and plants. J. Proteomics *109*, 400–416.
12. Leger, M.M., Gawryluk, R.M.R., Gray, M.W., and Roger, A.J. (2013). Evidence for a hydrogenosomal-type anaerobic ATP generation pathway in *Acanthamoeba castellanii*. PLoS ONE *8*, e69532.
13. Stechmann, A., Hamblin, K., Pérez-Brocal, V., Gaston, D., Richmond, G.S., van der Giezen, M., Clark, C.G., and Roger, A.J. (2008). Organelles in *Blastocystis* that blur the distinction between mitochondria and hydrogenosomes. Curr. Biol. *18*, 580–585.
14. de Graaf, R.M., Ricard, G., van Alen, T.A., Duarte, I., Dutilh, B.E., Burgtorf, C., Kuiper, J.W.P., van der Staay, G.W.M., Tielens, A.G.M., Huynen, M.A., and Hackstein, J.H. (2011). The organellar genome and metabolic potential of the hydrogen-producing mitochondrion of *Nyctotherus ovalis*. Mol. Biol. Evol. *28*, 2379–2391.
15. Brabender, M., Kiss, Á.K., Domonell, A., Nitsche, F., and Arndt, H. (2012). Phylogenetic and morphological diversity of novel soil cercomonad species with a description of two new genera (*Nucleocercomonas* and *Metabolomonas*). Protist *163*, 495–528.
16. Bass, D., Howe, A.T., Mylnikov, A.P., Vickerman, K., Chao, E.E., Edwards Smallbone, J., Snell, J., Cabral, C., Jr., and Cavalier-Smith, T. (2009). Phylogeny and classification of Cercomonadida (Protozoa, Cercozoa): *Cercomonas, Eocercomonas, Paracercomonas*, and *Cavernomonas* gen. nov. Protist *160*, 483–521.
17. Stairs, C.W., Eme, L., Brown, M.W., Mutsaers, C., Susko, E., Dellaire, G., Soanes, D.M., van der Giezen, M., and Roger, A.J. (2014). A SUF Fe-S cluster biogenesis system in the mitochondrion-related organelles of the anaerobic protist *Pygsuia*. Curr. Biol. *24*, 1176–1186.
18. Gill, E.E., Diaz-Triviño, S., Barberà, M.J., Silberman, J.D., Stechmann, A., Gaston, D., Tamas, I., and Roger, A.J. (2007). Novel mitochondrion-related organelles in the anaerobic amoeba *Mastigamoeba balamuthi*. Mol. Microbiol. *66*, 1306–1320.
19. de Graaf, R.M., Duarte, I., van Alen, T.A., Kuiper, J.W.P., Schotanus, K., Rosenberg, J., Huynen, M.A., and Hackstein, J.H.P. (2009). The hydrogenosomes of *Psalteriomonas lanterna*. BMC Evol. Biol. *9*, 287.
20. Pérez-Brocal, V., Shahar-Golan, R., and Clark, C.G. (2010). A linear molecule with two large inverted repeats: the mitochondrial genome of the stramenopile *Proteromonas lacertae*. Genome Biol. Evol. *2*, 257–266.
21. Akhmanova, A., Voncken, F., van Alen, T., van Hoek, A., Boxma, B., Vogels, G., Veenhuis, M., and Hackstein, J.H.P. (1998). A hydrogenosome with a genome. Nature *396*, 527–528.
22. von Heijne, G. (1986). Mitochondrial targeting sequences may form amphiphilic helices. EMBO J. *5*, 1335–1342.
23. Emanuelsson, O., Nielsen, H., Brunak, S., and von Heijne, G. (2000). Predicting subcellular localization of proteins based on their N-terminal amino acid sequence. J. Mol. Biol. *300*, 1005–1016.
24. Claros, M.G., and Vincens, P. (1996). Computational method to predict mitochondrially imported proteins and their targeting sequences. Eur. J. Biochem. *241*, 779–786.
25. Gabaldón, T., Rainey, D., and Huynen, M.A. (2005). Tracing the evolution of a large protein complex in the eukaryotes, NADH:ubiquinone oxidoreductase (Complex I). J. Mol. Biol. *348*, 857–870.
26. Brandt, U. (2006). Energy converting NADH:quinone oxidoreductase (complex I). Annu. Rev. Biochem. *75*, 69–92.
27. Vanlerberghe, G.C., and McIntosh, L. (1997). Alternative oxidase: from gene to function. Annu. Rev. Plant Physiol. Plant Mol. Biol. *48*, 703–734.
28. Pérez-Martínez, X., Antaramian, A., Vázquez-Acevedo, M., Funes, S., Tolkunova, E., d'Alayer, J., Claros, M.G., Davidson, E., King, M.P., and González-Halphen, D. (2001). Subunit II of cytochrome *c* oxidase in Chlamydomonad algae is a heterodimer encoded by two independent nuclear genes. J. Biol. Chem. *276*, 11302–11309.
29. Morales, J., Mogi, T., Mineki, S., Takashima, E., Mineki, R., Hirawake, H., Sakamoto, K., Ōmura, S., and Kita, K. (2009). Novel mitochondrial complex II isolated from *Trypanosoma cruzi* is composed of 12 peptides including a heterodimeric Ip subunit. J. Biol. Chem. *284*, 7255–7263.
30. Gawryluk, R.M.R., and Gray, M.W. (2010). An ancient fission of mitochondrial *Cox1*. Mol. Biol. Evol. *27*, 7–10.
31. Tanifuji, G., Archibald, J.M., and Hashimoto, T. (2016). Comparative genomics of mitochondria in chlorarachniophyte algae: endosymbiotic gene transfer and organellar genome dynamics. Sci. Rep. *6*, 21016.
32. Gutiérrez, P., Bulman, S., Alzate, J., Ortíz, M.C., and Marín, M. (2016). Mitochondrial genome sequence of the potato powdery scab pathogen *Spongospora subterranea*. Mitochondrial DNA A DNA Mapp. Seq. Anal. *27*, 58–59.
33. Lonjers, Z.T., Dickson, E.L., Chu, T.-P.T., Kreutz, J.E., Neacsu, F.A., Anders, K.R., and Shepherd, J.N. (2012). Identification of a new gene required for the biosynthesis of rhodoquinone in *Rhodospirillum rubrum*. J. Bacteriol. *194*, 965–971.
34. Brajcich, B.C., Iarocci, A.L., Johnstone, L.A.G., Morgan, R.K., Lonjers, Z.T., Hotchko, M.J., Muhs, J.D., Kieffer, A., Reynolds, B.J., Mandel, S.M., et al. (2010). Evidence that ubiquinone is a required intermediate

for rhodoquinone biosynthesis in *Rhodospirillum rubrum*. J. Bacteriol. *192*, 436–445.

35. Van Hellemond, J.J., Klockiewicz, M., Gaasenbeek, C.P.H., Roos, M.H., and Tielens, A.G.M. (1995). Rhodoquinone and complex II of the electron transport chain in anaerobically functioning eukaryotes. J. Biol. Chem. *270*, 31065–31070.

36. Gawryluk, R.M.R., Eme, L., and Roger, A.J. (2015). Gene fusion, fission, lateral transfer, and loss: Not-so-rare events in the evolution of eukaryotic ATP citrate lyase. Mol. Phylogenet. Evol. *91*, 12–16.

37. Des Rosiers, C., Fernandez, C.A., David, F., and Brunengraber, H. (1994). Reversibility of the mitochondrial isocitrate dehydrogenase reaction in the perfused rat liver. Evidence from isotopomer analysis of citric acid cycle intermediates. J. Biol. Chem. *269*, 27179–27182.

38. Xia, S., Frigo-Vaz, B., Zhao, X., Kim, J., and Wang, P. (2014). Biocatalytic carbon capture via reversible reaction cycle catalyzed by isocitrate dehydrogenase. Biochem. Biophys. Res. Commun. *452*, 147–150.

39. Möller, D., Schauder, R., Fuchs, G., and Thauer, R.K. (1987). Acetate oxidation to CO_2 via a citric acid cycle involving an ATP-citrate lyase: a mechanism for the synthesis of ATP via substrate level phosphorylation in *Desulfobacter postgatei* growing on acetate and sulfate. Arch. Microbiol. *148*, 202–207.

40. Bricker, D.K., Taylor, E.B., Schell, J.C., Orsak, T., Boutron, A., Chen, Y.-C., Cox, J.E., Cardon, C.M., Van Vranken, J.G., Dephoure, N., et al. (2012). A mitochondrial pyruvate carrier required for pyruvate uptake in yeast, *Drosophila*, and humans. Science *337*, 96–100.

41. Liaud, M.F., Lichtlé, C., Apt, K., Martin, W., and Cerff, R. (2000). Compartment-specific isoforms of TPI and GAPDH are imported into diatom mitochondria as a fusion protein: evidence in favor of a mitochondrial origin of the eukaryotic glycolytic pathway. Mol. Biol. Evol. *17*, 213–223.

42. Nakayama, T., Ishida, K., and Archibald, J.M. (2012). Broad distribution of TPI-GAPDH fusion proteins among eukaryotes: evidence for glycolytic reactions in the mitochondrion? PLoS ONE *7*, e52340.

43. Smith, D.G.S., Gawryluk, R.M.R., Spencer, D.F., Pearlman, R.E., Siu, K.W.M., and Gray, M.W. (2007). Exploring the mitochondrial proteome of the ciliate protozoon *Tetrahymena thermophila*: direct analysis by tandem mass spectrometry. J. Mol. Biol. *374*, 837–863.

44. van Grinsven, K.W.A., van Hellemond, J.J., and Tielens, A.G.M. (2009). Acetate:succinate CoA-transferase in the anaerobic mitochondria of *Fasciola hepatica*. Mol. Biochem. Parasitol. *164*, 74–79.

45. van Grinsven, K.W.A., Rosnowsky, S., van Weelden, S.W.H., Pütz, S., van der Giezen, M., Martin, W., van Hellemond, J.J., Tielens, A.G.M., and Henze, K. (2008). Acetate:succinate CoA-transferase in the hydrogenosomes of *Trichomonas vaginalis*: identification and characterization. J. Biol. Chem. *283*, 1411–1418.

46. Marvin-Sikkema, F.D., Driessen, A.J.M., Gottschal, J.C., and Prins, R.A. (1994). Metabolic energy generation in hydrogenosomes of the anaerobic fungus *Neocallimastix*: evidence for a functional relationship with mitochondria. Mycol. Res. *98*, 205–212.

47. Youssef, N.H., Couger, M.B., Struchtemeyer, C.G., Liggenstoffer, A.S., Prade, R.A., Najar, F.Z., Atiyeh, H.K., Wilkins, M.R., and Elshahed, M.S. (2013). The genome of the anaerobic fungus *Orpinomyces* sp. strain C1A reveals the unique evolutionary history of a remarkable plant biomass degrader. Appl. Environ. Microbiol. *79*, 4620–4634.

48. Schneider, R.E., Brown, M.T., Shiflett, A.M., Dyall, S.D., Hayes, R.D., Xie, Y., Loo, J.A., and Johnson, P.J. (2011). The *Trichomonas vaginalis* hydrogenosome proteome is highly reduced relative to mitochondria, yet complex compared with mitosomes. Int. J. Parasitol. *41*, 1421–1434.

49. Tielens, A.G.M., van Grinsven, K.W.A., Henze, K., van Hellemond, J.J., and Martin, W. (2010). Acetate formation in the energy metabolism of parasitic helminths and protists. Int. J. Parasitol. *40*, 387–397.